ACS Infectious Diseases

pubs.acs.org/journal/aidcbc

Article

Development of Host-Cleavable Antibody−Bactericide Conjugates against Extracellular Pathogens

Meghan K. O'Leary, Asraa Ahmed, and Christopher A. Alabi*

Cite This: https://doi.org/10.1021/acsinfecdis.2c00492

Read Online

ACCESS | Metrics & More | Article Recommendations | Supporting Information

ABSTRACT: Novel antimicrobial agents with potent bactericidal activity are needed to treat infections caused by multidrug-resistant (MDR) extracellular pathogens, such as *Pseudomonas aeruginosa*. Antimicrobial peptides (AMPs) and peptidomimetics are promising alternatives to traditional antibiotics, but their therapeutic use is limited due to the lack of specificity and resulting off-target effects. The incorporation of an antibody into the drug design would alleviate these challenges by localizing the AMP to the target bacterial cells. Antibody−drug conjugates (ADCs) have already achieved clinical success as anticancer therapeutics, due to the ability of the antibody to deliver the payload directly to the cancer cells. This strategy involves the selective delivery of highly cytotoxic drugs to the target cells, which enables a broad therapeutic window. This platform can be translated to the treatment of infections, whereby an antibody is used to deliver an antimicrobial agent to the bacterial antigen. Herein, we propose the development of an antibody−bactericide conjugate (ABC) in which the antibacterial oligothioetheramide (oligoTEA), BDT-4G, is coupled to an anti-*P. aeruginosa* antibody via a cleavable linker. The drug BDT-4G was chosen based on its efficacy against a range of *P. aeruginosa* isolates and its ability to evade mechanisms conferring resistance to the last-resort agent polymyxin B. We demonstrate that the ABC binds to the bacterial cell surface, and following cleavage of the peptide linker, the oligoTEA payload is released and exhibits antipseudomonal activity.

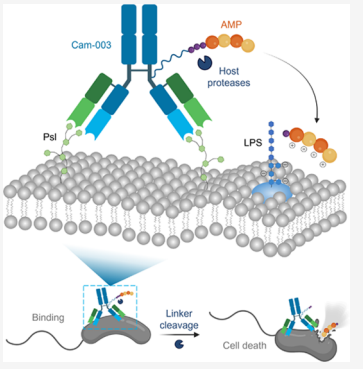

KEYWORDS: *antibody-drug conjugate, antimicrobial peptide, extracellular pathogens, multidrug resistance, Pseudomonas aeruginosa*

The growing prevalence of multidrug-resistant (MDR) extracellular pathogens has rendered many antibiotics ineffective. This presents a global health crisis and motivates the need to develop new antimicrobial strategies. Small-molecule drugs comprise the majority of traditional antibiotics; however, many of them only have an ∼10-year life span post-discovery before resistant bacterial isolates emerge.[1] Consequently, novel antimicrobials with potent activity against these MDR isolates must be developed, but the challenge lies in discovering antimicrobial compounds specific to bacterial cells. Unconventional antimicrobial strategies, such as antimicrobial peptides (AMPs) and their mimetics, antibodies, and antibody−drug conjugates (ADCs), represent a relatively untapped depot of alternative antibiotic therapeutics.

Until recently, antibody and ADC therapeutics have been mostly employed for cancer treatment, and this platform has yet to be fully harnessed for use against bacterial infections. Similar to antitumor effects, antibodies can exert antimicrobial effects through direct toxin neutralization, complement-dependent cytotoxicity (CDC), antibody-dependent cellular cytotoxicity (ADCC), or antibody-dependent cellular phagocytosis (ADCP).[2,3] Monoclonal antibodies (mAbs) possess an advantage over many traditional antibiotics in that they are less likely to promote resistance due to their indirect mechanism of killing, and owing to their species specificity, they do not disrupt the gut microbiome.[4] To be an effective therapeutic, the mAb should bind to a bacterial target that is conserved across strains and is vital to the fitness of the cell to impede the development of resistance.[5]

Serotype-independent targets have been identified for several bacteria that pose a serious clinical threat.[6−8] For example, the exopolysaccharide Psl is conserved across the majority of *Pseudomonas aeruginosa* clinical isolates.[8] Out of 173 clinical isolates of *P. aeruginosa* from a range of infection types, Psl was expressed in 96% of the isolates from nonchronic infections and in 73% of the isolates obtained from the lungs of patients with cystic fibrosis.[7] Psl is a neutral, branched pentasaccharide that contributes to the virulence of *P. aeruginosa* due to its involvement in host cell attachment and the formation and maintenance of biofilms.[4,9] In addition, Psl inhibits complement-mediated opsonization, and this immune evasion mechanism protects the bacterial cell from phagocytic death.[10] As such, antibodies that target Psl may augment immune recognition and clearance of *P. aeruginosa*.

Cam-003 is a monoclonal antibody developed by MedImmune (AstraZeneca) that binds to Psl with a K_D of 144 nM.[7]

Received: September 29, 2022

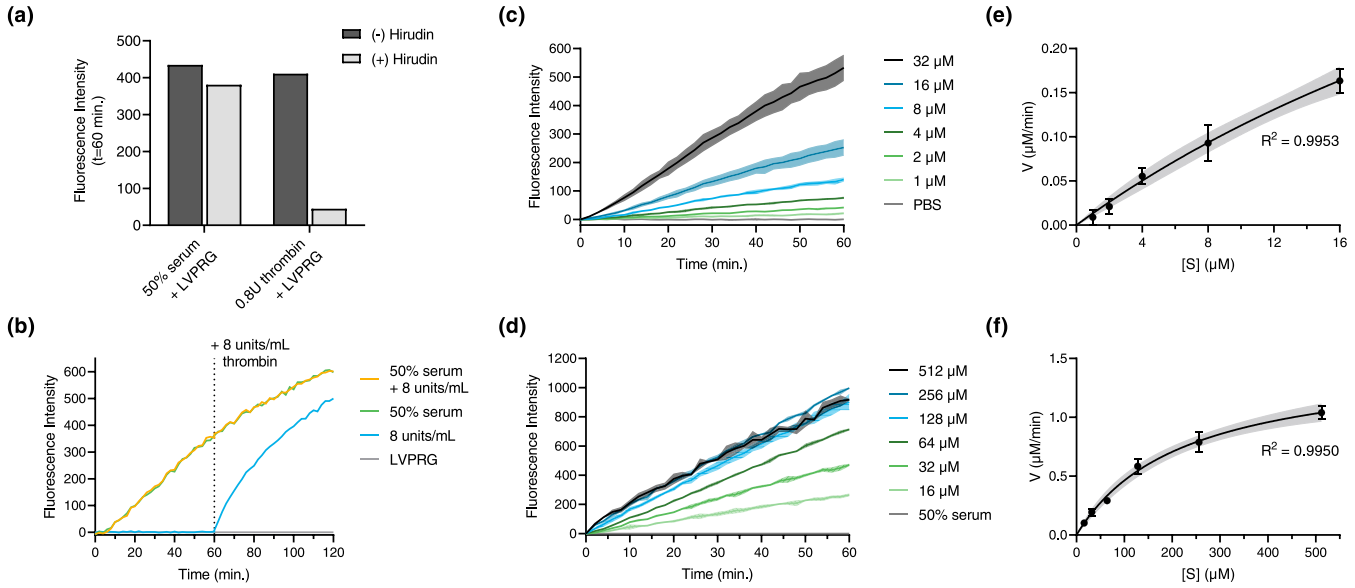

Figure 1. (a) Relative fluorescence intensity after 60 min of LVPRG (16 μM) incubated with 50% normal mouse serum and 8 units/mL thrombin with or without 2.5 equiv hirudin (with respect to thrombin). (b) Addition of 8 units/mL thrombin after 60 min incubation of the peptide alone or in 50% mouse serum. Fluorescence intensity of different concentrations of fluorogenic LVPRG incubated in (c) 40 units/mL thrombin or (d) 50% serum for 1 h at 37 °C. The concentration of the peptide substrate, [*S*], versus the initial rate of cleavage, *V*, in (e) thrombin and (f) serum. For (c)−(f), averages (n = 2) are represented by solid lines and standard deviations are represented by shaded bands.

Cam-003 was discovered from a single-chain variable fragment (scFv) phage display library derived from healthy humans.[7] Cam-003 has demonstrated potent opsonophagocytic killing of *P. aeruginosa in vitro*, as well as the ability to inhibit PAO1 attachment to A549 human lung epithelial cells.[7] Most notably, Cam-003 has protected against *P. aeruginosa* infection in mouse models of acute pneumonia, thermal injury, and ocular keratitis when administered intraperitoneally 24 h before infection.[7] However, the ability of Cam-003 to treat established infections has not been reported and thus, may only have utility as a preventative therapy. Furthermore, Cam-003 has yet to be explored as a vehicle for the targeted delivery of bactericidal drugs to infectious *P. aeruginosa*.

Nontraditional chemical agents that target anionic lipids in the bacterial cell membrane, such as AMPs, facilitate cell death via bilayer disruption.[11] Despite their potency and promise, AMPs have yet to enjoy broad clinical success, primarily due to their lack of systemic specificity and off-target effects *in vivo*.[12−14] We hypothesize that specificity to bacteria such as *P. aeruginosa* can be induced by targeting AMPs and their mimetics directly to *P. aeruginosa* cells via the use of a *P. aeruginosa*-specific antibody to create an antibody−bactericide conjugate (ABC). The advantage of this ABC strategy over traditional antibiotics is that the antibody can directly deliver the potent antibacterial agent to the invading pathogen at higher local concentrations, and this localization has the potential to increase the efficacy of the payload and mitigate off-target effects.

For proof of concept of this ABC platform, Cam-003 will be conjugated to the bactericidal agent BDT-4G. BDT-4G is a sequence-defined, cationic 4-mer from the oligothioetheramide (oligoTEA) class of AMP mimetics. BDT-4G has displayed potent activity against a range of *P. aeruginosa* clinical isolates, including meropenem- and polymyxin-resistant isolates.[15] However, BDT-4G is currently dose-limited *in vivo* due to its inherent toxicity conferred by its cationic charge. Hence, the incorporation of BDT-4G into an ABC has the potential to reduce the off-target effects and potentiate the bactericidal activity of the oligoTEA. In this design, BDT-4G is conjugated to Cam-003 via a host-cleavable LVPRG peptide linker. The LVPRG linker was chosen to exploit the activation of the blood coagulation system that occurs during bacterial infections.[16] Particularly, LVPRG can be cleaved by thrombin, which is upregulated during infections to limit the spread of bacteria and enhance the host defense through mechanisms including fibrin polymerization and platelet−neutrophil interactions.[17−20]

RESULTS

Validation of a Peptide Substrate as the Host-Cleavable ABC Linker. To assess conditions under which the LVPRG linker cleaves, fluorescence resonance energy transfer (FRET) assays were performed using a fluorogenic derivative of the peptide (Dabcyl-LVPRG-Edans). The peptide was incubated at 16 μM in 1× PBS at 37 °C with varying concentrations of normal mouse serum and thrombin from human plasma, and the fluorescence intensity was measured for 60 min at an excitation of 340 nm and an emission of 500 nm (Figure S1). Under all conditions, there was an increase in the relative fluorescence intensity, which is proportional to the amount of cleaved substrate, and therefore indicates that LVPRG is cleaved by both serum and thrombin. To assess whether thrombin was responsible for cleavage of the linker in serum, the samples were co-incubated with hirudin, a naturally occurring thrombin inhibitor from the salivary glands of blood-sucking leeches, and the fluorescence intensity was measured over time.[21] The addition of ≥2.5 equiv of hirudin (with respect to 8 units/mL thrombin) resulted in successful inhibition of thrombin proteolytic activity (Figures 1a and S2a). However, up to 25 equiv of hirudin was not able to prevent cleavage of the peptide in serum, indicating that other proteases are responsible for serum-mediated cleavage of LVPRG (Figures 1a and S2b).

https://doi.org/10.1021/acsinfecdis.2c00492
ACS Infect. Dis. XXXX, XXX, XXX−XXX

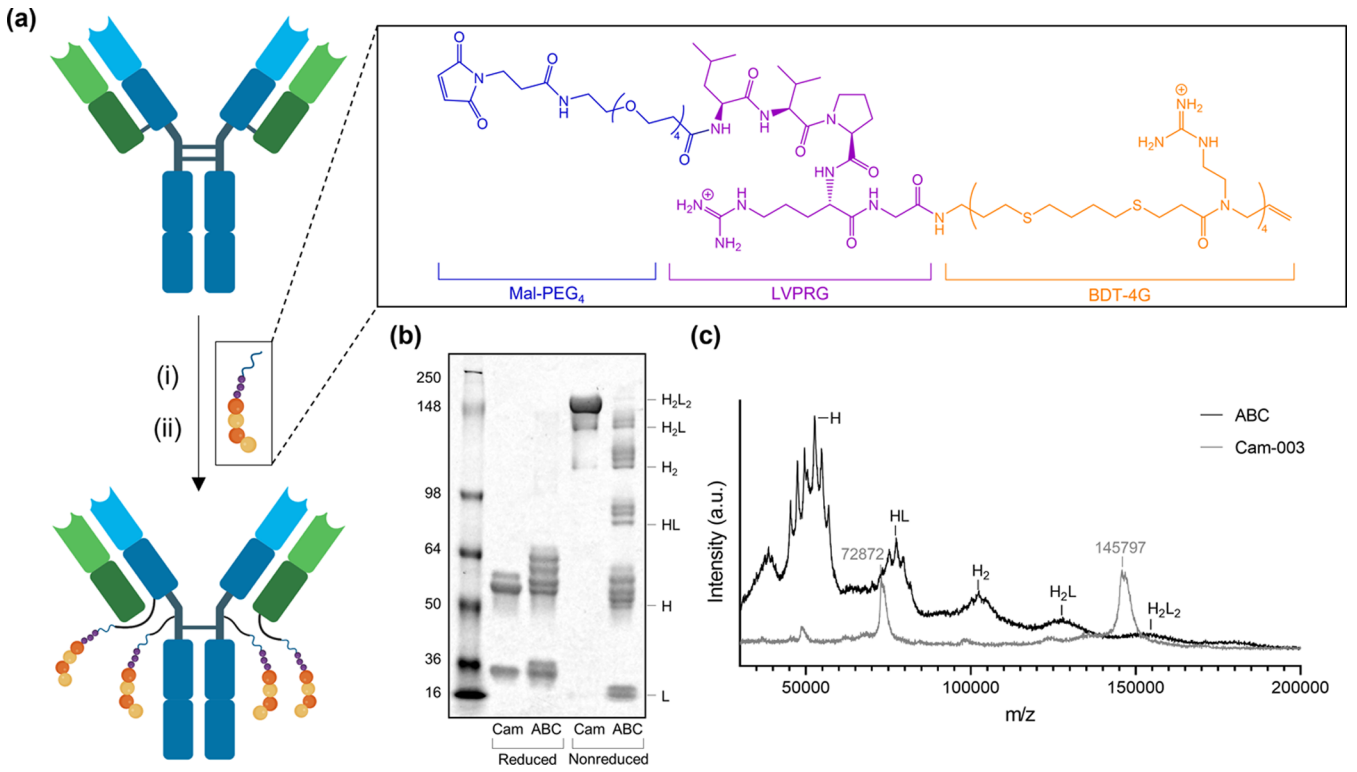

Figure 2. (a) Assembly of ABC: (i) 4.2 equiv TCEP, 2 h at 37 °C, (ii) 10 equiv Mal-PEG$_4$-LVPRG-BDT-4G, r.t., overnight. (b) SDS-PAGE gel of Cam-Mal-PEG$_4$-LVPRG-BDT-4G (ABC) under reducing and nonreducing conditions compared to unmodified Cam-003. (c) MALDI-TOF MS of native Cam-Mal-PEG$_4$-LVPRG-BDT-4G (ABC) and Cam-003; 145797 Da corresponds to the full mass of the antibody, [M + H$^+$], and 72872 Da corresponds to the half-mass, [M + 2H$^+$]/2. In (b) and (c), H refers to the heavy chain and L refers to the light chain.

To evaluate if the addition of thrombin increases the rate of cleavage, serum was spiked with thrombin after 60 min of preincubation with the peptide and the fluorescence intensity was measured for an additional hour. The fluorescence intensity of the spiked serum sample did not increase relative to serum without thrombin, indicating that the rate of cleavage is slower (or the same) in thrombin under these conditions (Figure 1b). Serum spiked with thrombin at the onset of the experiment also did not enhance the cleavage of LVPRG (Figure S2c). To determine if the fluorescence intensity plateaued over longer periods, which would signify the complete extent of cleavage, 16 μM of the fluorogenic peptide was incubated with either 50% serum or 8 units/mL thrombin and the fluorescence was recorded for 4 h. Both the serum and thrombin samples approached a plateau at 4 h, which suggests that cleavage was progressing to completion (Figure S2d).

The kinetic parameters of the protease-peptide system were determined by incubating various concentrations of the fluorogenic peptide with 40 units/mL thrombin and 50% mouse serum at 37 °C and recording the fluorescence intensity for 1 h (Figure 1c,d). The concentration of the peptide substrate, [S], versus the initial rate of cleavage, V, were plotted (Figure 1e,f), and the following kinetic parameters were calculated by fitting the data to the Michaelis−Menten equation using nonlinear regression: V_{max} = 0.661 μM/min, K_m = 48.6 μM, and k_{cat}/K_m = 654 M^{-1} s^{-1} for 40 units/mL of thrombin, and V_{max} = 1.49 μM/min and K_m = 222 μM for 50% mouse serum. While the catalytic efficiency (k_{cat}/K_m) cannot be compared due to the unknown serum protease concentration, the data show a 4-fold lower K_m for thrombin than serum proteases, indicating that LVPRG has a stronger affinity for thrombin than general serum proteases.

Synthesis and Characterization of ABCs. BDT-4G was synthesized as previously described.[15] The drug conjugate was synthesized by coupling the C-terminus of the LVPRG linker to the free primary amine on BDT-4G (Scheme S1 and Figure S3) and then conjugating a maleimide group (Mal) to the N-terminus of the peptide via a short PEG$_4$ linker (Scheme S2 and Figure S4). To determine the location of linker cleavage, the conjugate was incubated in 40 units/mL thrombin or 50% serum for 4 h at 37 °C and the cleavage fragments were analyzed via MALDI-TOF MS. Both thrombin and serum cleaved the linker after the arginine residue (Figure S6), which leaves a glycine residue attached to BDT-4G. However, we demonstrate that this remaining amino acid has a minimal effect on the antimicrobial activity of BDT-4G (Figure S7).

The antibody−bactericide conjugate (ABC) was synthesized according to the reaction pathway in Figure 2a and Scheme S4. The ABC was characterized via SDS-PAGE under both reducing and nonreducing conditions. All samples were heated for 5 min at 95 °C and run on a 7.5% polyacrylamide gel using Tris/Gly/SDS running buffer at 100 V for 70 min (Figure 2b). Cam-003 showed a double band at the heavy chain region (~50 kDa) of the reduced sample, which is indicative of heterogeneous glycosylation. This hypothesis is supported by the double peaks that are present in both the MALDI-TOF MS spectrum (~146 kDa, Figure 2c) and the analytical HIC trace (Figure S8). The reduced ABC had multiple bands at both ~50 and ~25 kDa, which is indicative of drug conjugation to both the heavy and light chains, respectively. Under nonreducing conditions, Cam-003 displays the main

https://doi.org/10.1021/acsinfecdis.2c00492
ACS Infect. Dis. XXXX, XXX, XXX−XXX

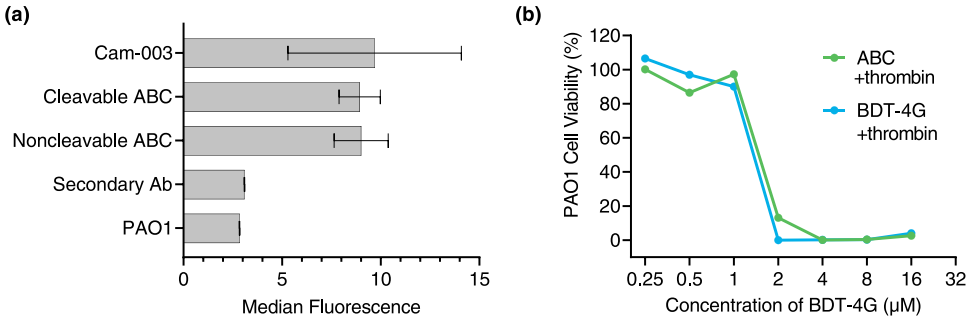

Figure 3. (a) Median fluorescence to detect binding of 62.5 nM Cam-003, cleavable ABC, and noncleavable ABC to *P. aeruginosa* isolate PAO1 after 1 h incubation at 4 °C and compared to the fluorescent secondary antibody and PAO1 alone. Error bars represent the standard deviation (n = 2). (b) Percent cell viability of *P. aeruginosa* isolate PAO1 exposed to increasing concentrations of Cam-Mal-PEG$_4$-LVPRG-BDT-4G (ABC, DAR 3.8) and BDT-4G in the presence of 64 units/mL thrombin. Concentration corresponds to the μM of BDT-4G and accounts for the DAR.

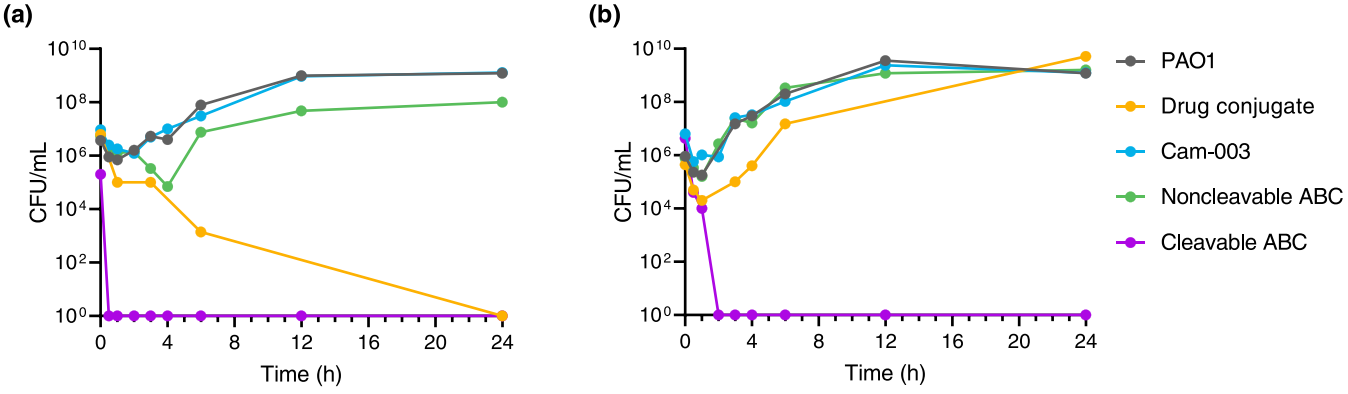

Figure 4. (a) Kill curve and (b) bind-kill curve assays, the latter which is designed to contain only membrane-bound material, of 16 μM Mal-PEG$_4$-LVPRG-BDT-4G (drug conjugate), Cam-003, Cam-Mal-PEG$_4$-BDT-4G (noncleavable ABC, DAR = 3.6, corresponding to 57.6 μM BDT-4G), and Cam-Mal-PEG$_4$-LVPRG-BDT-4G (cleavable ABC, DAR = 3.8, corresponding to 60.8 μM BDT-4G) with 40 units/mL thrombin against *P. aeruginosa* isolate PAO1.

band at ∼146 kDa, which corresponds to the full-length antibody (2 heavy chains and 2 light chains, H_2L_2) and a lighter band at ∼125 kDa, which is consistent with the mAb lacking a single light chain (H_2L) and can be attributed to the antibody production process.[22] The peak at ∼75 kDa represents the half-mass of the full mAb. The ABC has six distinct regions of bands at ∼150, 125, 100, 75, 50, and 25 kDa, which correlate with H_2L_2, H_2L, H_2, HL, H, and L, respectively. The faint band at 150 kDa corroborates disruption of the interchain disulfide bridges due to conjugation to the reduced cysteine residues and indicates that noncovalent interactions (ionic, hydrogen bonds, van der Waals, hydrophobic) can no longer hold the antibody together under the harsh conditions of SDS.[23] The multiple bands in these regions further support the hypothesis that the payload has been conjugated to both the heavy and light chains. In addition, these bands provide evidence that the payload conjugation sites are heterogeneous, as H_2L (125 kDa) and H_2 (100 kDa) substantiate an intact hinge region, and thus coupling to the Fab region, whereas HL (75 kDa) and H (50 kDa) support conjugation to the core hinge. The MALDI-TOF mass spectrum confirms the presence of conjugated H_2L_2, H_2L, H_2, HL, H, and L fragments (Figure 2c). A DAR of 3.8 was calculated using the difference in the full-length mass-to-charge ratio (m/z) between the ABC and unmodified Cam-003 (Figure 2c).

The noncleavable ABC control, Cam-Mal-PEG$_4$-BDT-4G, was generated by first synthesizing the noncleavable drug conjugate, Mal-PEG$_4$-BDT-4G (Scheme S3), and then coupling the purified payload (Figure S5) to the reduced disulfide bridges of Cam-003 (Scheme S5). The resulting noncleavable ABC was characterized via SDS-PAGE and MALDI-TOF MS to yield a DAR of 3.6 (Figures S9 and S10).

Binding of ABCs to *P. aeruginosa*. After the synthesis and characterization of the ABCs, the effect of the oligoTEA payload on antibody−antigen binding was assessed given the presence of multiple conjugated antibody fragments. Unmodified Cam-003, the cleavable ABC (Cam-Mal-PEG$_4$-LVPRG-BDT-4G), and the noncleavable ABC (Cam-Mal-PEG$_4$-BDT-4G) were all incubated with *P. aeruginosa* reference isolate PAO1 at 62.5 nM for 1 h at 4 °C to allow for binding. Next, a fluorescent secondary antibody that binds to the Fc region of human IgG was added to the samples for 30 min. The cells were fixed in 4% paraformaldehyde, washed in 1× PBS, and the fluorescence was measured via flow cytometry. The binding of the ABCs was compared to PAO1 cells alone, as well as the fluorescent secondary antibody incubated with PAO1 to normalize for nonspecific interactions between the secondary antibody and the bacterial cells. Both the cleavable and noncleavable ABC exhibited a median fluorescence and a fluorescence histogram that was similar to Cam-003 (Figure 3a). Thus, it appears that conjugation does not negatively impact the binding of the ABC to the bacterial cells even though evidence suggests that BDT-4G may be coupled to the reduced disulfides of the Fab region (Figure 2).

https://doi.org/10.1021/acsinfecdis.2c00492
ACS Infect. Dis. XXXX, XXX, XXX−XXX

Antimicrobial Activity of ABCs Against *P. aeruginosa*. To assess the antimicrobial activity of the ABC against *P. aeruginosa*, the cleavable ABC (Cam-Mal-PEG_4-LVPRG-BDT-4G) was co-incubated with 64 units/mL thrombin and bacteria cells, and cell viability was determined via a minimum inhibitory concentration (MIC) assay. Incubation of the ABC in thrombin resulted in full recovery of antimicrobial activity similar to BDT-4G (Figure 3b). To evaluate the bactericidal activity of the ABCs against *P. aeruginosa*, a kill curve assay was performed (Figure 4a) following the previously described protocol.[15] The nontargeted drug conjugate (Mal-PEG_4-LVPRG-BDT-4G), unmodified Cam-003, noncleavable ABC (DAR = 3.6), and cleavable ABC (DAR = 3.8) were all tested at 16 μM, corresponding to a BDT-4G concentration of 57.6 and 60.8 μM for the noncleavable and cleavable ABCs, respectively. All samples were co-incubated with 40 units/mL thrombin, and bactericidal activity was defined as a 3-log reduction (i.e., 10^3) of PAO1 CFU/mL. Under these conditions, the cleavable ABC was bactericidal within 30 min and the cleavable (nontargeted) drug conjugate killed all bacteria (6-log reduction), albeit slowly, within 24 h. The noncleavable ABC exhibited a modest bactericidal effect, which rapidly waned with time (1-log reduction at t = 24 h). As expected, Cam-003 was inactive since the effector functions of the mAb depend on interactions between the Fc domain and immune effector cells, which were absent in this *in vitro* assay.

The combined events of antibody−antigen binding, linker cleavage, and oligoTEA-mediated bacterial cell lysis were evaluated via a novel bind-kill kinetics assay (Figure 4b). Compounds at 16 μM were first preincubated with 5×10^6 CFU/mL of *P. aeruginosa* isolate PAO1 for 30 min at room temperature to allow for antibody binding to the bacterial cell surface. Samples were then centrifuged, and the supernatant was immediately removed, thus removing any compounds that were not bound to the cells. The remaining cell pellet, which contained membrane-bound material, was resuspended, 40 units/mL of thrombin was added to the culture, and a time-kill curve kinetics assay was performed as described above. Cam-Mal-PEG_4-LVPRG-BDT-4G killed all bacteria within 2 h (6-log reduction), indicating that the ABC is able to bind to the bacterial cells at a concentration greater than or equal to the minimum bactericidal concentration, release the payload via cleavage of the linker by thrombin, and exert bactericidal effects through oligoTEA-mediated permeabilization of the bacterial cell membrane. In a subsequent biological replicate, the cleavable ABC killed all bacteria within 30 min (Figure S11). The drug conjugate, Mal-PEG_4-LVPRG-BDT-4G, which was active in the preceding kill curve (Figure 4a), was no longer bactericidal in the bind-kill assay, substantiating the effect of antibody targeting. Both Cam-003 and the noncleavable ABC were inactive in the bind-kill assay, but this was due to a lack of antimicrobial activity, not an inability to bind to the bacterial cells (Figure 3a).

DISCUSSION

The oligoTEA BDT-4G is a potent bactericidal agent against *P. aeruginosa* that exerts its mechanism of action via permeabilization and destabilization of the bacterial cell membrane.[15] However, the cationic charge of this oligoTEA, which allows BDT-4G to interact electrostatically with the negatively charged bacterial cell membrane, also imparts toxicity against mammalian cells, which contain some anionic lipids but generally have a neutral surface charge.[24] Therefore, in its present form, BDT-4G is unsuitable for systemic applications. In parallel, the monoclonal antibody Cam-003 has been shown to protect against *P. aeruginosa* infections *in vivo*; however, its efficacy as a post-infection treatment is currently unknown.[7] As such, BDT-4G and Cam-003 can be coupled together to produce an antibody−bactericide conjugate (ABC) that combines the favorable properties of each constituent (bactericidal activity and antigen targeting, respectively), while balancing the less desirable attributes (lack of specificity of BDT-4G and indirect antibacterial activity of Cam-003).

To couple BDT-4G to Cam-003, we investigated the LVPRG peptide as a host-cleavable linker. Cleavage of LVPRG by both mouse serum and thrombin was confirmed via FRET assays (Figures 1, S1, and S2), and in future studies, the cleavage kinetics can be tuned to ensure the payload is released after Cam-003 binds to Psl *in vivo*, to prevent premature systemic release of a lytic agent. To synthesize the drug conjugate, the C-terminus of LVPRG was coupled to the backbone primary amine of BDT-4G and then a maleimide group (Mal-PEG_4) was attached to the free N-terminus of the peptide to allow for antibody binding. The purified drug conjugate, Mal-PEG_4-LVPRG-BDT-4G, was then coupled to the reduced disulfides of Cam-003 and an average DAR of 3.8 was determined via MALDI-TOF MS (Figure 2c). The ABC was further characterized with SDS-PAGE under both reducing and nonreducing conditions, which gave evidence of a heterogeneous ABC that varies in the payload conjugation site (Figure 2b). In future work, site-specific conjugation strategies can be explored to control the conjugation site and DAR, for example, by introducing functional handles on the antibody through recombinant engineering or through enzyme-mediated approaches.[25,26]

Though the nonreducing SDS-PAGE gel corroborated drug conjugation to the Fab region, the binding of the ABC to *P. aeruginosa* was not inhibited by the oligoTEA payload (Figure 3a). The antimicrobial activity of the ABC against *P. aeruginosa* was evaluated through *in vitro* time-kill studies to reveal effective linker cleavage with the addition of thrombin and subsequent potent bactericidal effects (Figure 4a). The activity of the ABC was also compared to that of unmodified Cam-003 and a noncleavable ABC control, Cam-Mal-PEG_4-BDT-4G, both of which were inactive. The inactivity of Cam-003 was expected, as the antibody has an indirect mechanism of bacterial killing that requires effector cells associated with the host immune response to phagocytose *P. aeruginosa*.

Next, ABC binding and antimicrobial activity were evaluated in parallel via binding time-kill experiments (Figures 4b and S11). In these experiments, the ABC or controls were allowed to bind to the bacteria for 30 min after which the culture was centrifuged, the supernatant was discarded to remove any unbound compounds, the pellet was resuspended, and a time-kill curve assay was performed. Through these studies, it was shown that the ABC is able to bind to the bacteria and subsequently exert its bactericidal activity. In comparison, the drug conjugate alone, unmodified Cam-003, and the noncleavable ABC control were all inactive. The lack of activity of the drug conjugate is due to its inability to bind to *P. aeruginosa*, while Cam-003 and the noncleavable ABC bind but lack antimicrobial activity under experimental conditions.

In preparation for *in vivo* studies, we evaluated the activity of the ABC in the presence of host proteases. While the ABC regained full activity with the addition of thrombin in bacterial culture media (Figure 3b), bactericidal activity was only

https://doi.org/10.1021/acsinfecdis.2c00492
ACS Infect. Dis. XXXX, XXX, XXX−XXX

partially regained in the combined presence of thrombin and 50% serum (Figure S12a). To assess the effect of serum and thrombin on antimicrobial activity, unmodified BDT-4G and *P. aeruginosa* were co-incubated with 50% mouse serum or 64 units/mL thrombin and bacterial cell viability was assessed via a MIC assay. Similar to the drug conjugate, BDT-4G retained antimicrobial activity when incubated with thrombin (Figure 3b) but was inhibited in the presence of serum (Figure S12b). As thrombin has been measured to be ∼851 nM (98 units/mL) in healthy humans during the propagation phase of the clotting process, the concentrations of thrombin used herein are predicted to be clinically relevant.[27] Thrombin and mouse serum were then individually incubated with *P. aeruginosa* at various concentrations to reveal that both had minimal impact on cell viability (Figure S13a,b). However, when the cell counts from the serum MIC assay were enumerated, higher concentrations of serum resulted in an order of magnitude more CFU/mL of *P. aeruginosa*, suggesting that the addition of 50% serum may supplement bacterial growth (Figure S13c). Further studies are underway to fully understand the serum effect on these conjugates.

This ABC approach is the first-in-class antibody-targeted membrane-permeabilizing bactericide conjugate focused on treating extracellular infections. This work was inspired by the antibody−antibiotic conjugate (AAC) introduced by Genentech in 2015 to eliminate intracellular *Staphylococcus aureus*.[28] AACs are composed of an anti-*S. aureus* antibody conjugated via a cathepsin-cleavable linker to the antibiotic rifalogue that is activated only after it is taken up by macrophages and released in the proteolytic environment of the phagolysosome. AACs differ from our ABCs in that they only kill engulfed intracellular bacteria after phagolysosomal cathepsin cleavage of the valine-citrulline linker. The ABCs proposed in this work are designed to bind to bacteria, cleave, and release the AMP mimetic in the extracellular environment to exert its bactericidal activity. Unlike AACs that require a competent immune system, an innovative feature of this work is that ABCs are designed to be active even in an immunocompromised host that lacks the essential immune cells that contribute to host defense during infection. In addition, as Cam-003 has been shown in the literature to only bind to Psl-presenting *P. aeruginosa* (as opposed to PAO1Δ*pslA*), we hypothesize that the ABC will be able to differentiate between microbial species.[7] Finally, given the targeted nature of the ABC, we also anticipate a minimized disruption to the gut microbiome, an advantage over traditional small-molecule antibiotics, which can have a severe impact on the diversity of microbial species in the microbiome.

CONCLUSIONS

Herein, we have demonstrated proof of concept of the antibody−bactericide conjugate platform for the targeted delivery of AMP mimetics to invading pathogens. In this design, the oligoTEA BDT-4G was coupled to the Cam-003 mAb via the LVPRG peptide, and the kinetics of linker cleavage were elucidated via FRET. The resulting ABC was characterized via MALDI-TOF MS and SDS-PAGE and was shown to effectively bind to *P. aeruginosa*, unhindered by the oligoTEA payload. The ABC inhibited growth of *P. aeruginosa* when co-incubated with thrombin, and at a DAR of 3.8, the ABC decreased *P. aeruginosa* bacterial counts by 10^6 within 30 min of exposure. In an original bind-kill assay, the ABC was able to bind to the bacterial cells and subsequently exert bactericidal effects, resulting in a 10^6 decrease in bacterial counts within 2 h. Taken together, these studies support the ABC strategy for the treatment of extracellular bacterial infections. Future work will involve tuning the linker to achieve optimal cleavage kinetics and investigating serum effects on ABC efficacy prior to *in vivo* studies. Success of this ABC strategy *in vivo* will open the door to using a wide range of potent AMPs and AMP mimetics that have been discarded due to unfavorable physicochemical properties, such as toxicity or insolubility. Thus, through this platform, drugs can be repurposed to provide alternative therapeutics to treat infections caused by extracellular pathogens.

METHODS

Materials and Instrumentation. Fmoc-LVPRG-OH was synthesized using a Liberty Blue Microwave Peptide Synthesizer (CEM) and purified via high-performance liquid chromatography (HPLC). Cam-003 was purchased from Creative Biolabs (MRO-160MZ). The fluorogenic peptide, Dabcyl-LVPRG-Edans, was purchased from GenScript Biotech. Normal mouse serum was purchased from Thermo Fisher Scientific (10410), thrombin from human plasma was purchased from Sigma-Aldrich (T6884), and hirudin from leeches was also purchased from Sigma-Aldrich (H7016). Granulated LB broth was purchased from Research Products International, and centrifugal filter units were purchased from Sigma-Aldrich.

FRET assays were performed using a TECAN Infinite M1000 PRO Microplate Reader (Männdorf, Switzerland). PAGE was performed on a Mini-PROTEAN Electrophoresis System (Bio-Rad Laboratories) using a 7.5% precast polyacrylamide gel and Tris/Glycine/SDS running buffer. LCMS characterization was performed on an Agilent 1100 LCMS system (single-quad G1956B) in positive-ion mode using a Poroshell 120 EC-C18 column (3 mm × 100 mm, 2.7 μm) purchased from Agilent Technology, with absorbance recorded at 210, 230, 260, 360, and 566 nm. Samples were analyzed on a gradient of 5−100% acetonitrile in water with 0.1% acetic acid and were eluted at a flow rate of 0.6 mL/min. HPLC purification was performed on an Agilent 1100 Series HPLC system equipped with a UV diode array detector and an 1100 Infinity analytical scale fraction collector. Tabulated data were processed with GraphPad Prism 9.4.0 (673).

Synthesis of Mal-PEG$_4$-LVPRG-BDT-4G. Fmoc-LVPRG-OH (1 equiv) was reacted with 1.2 equiv HBTU and 3 equiv DIPEA in 50 mM dry DMF for 15 min at room temperature, after which *N*-hydroxysuccinimide (1.2 equiv) was added and the reaction was allowed to proceed for an additional hour. BDT-4G was then added directly to the reaction mixture at a concentration that corresponded to an excess of Fmoc-LVPRG-NHS (2 equiv), and the reaction proceeded overnight at room temperature. For Fmoc deprotection, 60% v/v diethylamine was added, and the mixture was reacted for 90 min. LVPRG-BDT-4G (Scheme S1) was purified via HPLC using a semipreparative reversed-phase C18 column (9.4 mm × 250 mm, 5 μm) and was eluted at a flow rate of 4 mL/min. The mobile phase consisted of acetonitrile with 0.1% v/v TFA (solvent A) and water with 0.1% v/v TFA (solvent B). The linear solvent gradient consisted of 5−35% solvent A for 5 min, followed by 35−47% solvent A for 20 min. LVPRG-BDT-4G was eluted at 37.5% solvent A (9.1 min), and the product was confirmed with MALDI-TOF MS (Figure S3).

https://doi.org/10.1021/acsinfecdis.2c00492
ACS Infect. Dis. XXXX, XXX, XXX−XXX

Purified LVPRG-BDT-4G was then functionalized with a maleimide group by reacting it with 2 equiv monodisperse Mal-dPEG$_4$-NHS ester (Quanta BioDesign, Ltd.) and 20 equiv TEA in dry DMSO for 2 h at room temperature (Scheme S2). Mal-PEG$_4$-LVPRG-BDT-4G was purified using an analytical reversed-phase C18 column (4.6 mm× 150 mm, 5 μm) and was eluted at a flow rate of 1 mL/min. The linear solvent gradient consisted of 5−30% solvent A for 5 min, followed by 30−60% solvent A for 20 min. Mal-PEG$_4$-LVPRG-BDT-4G eluted at 40.6% solvent A (12.1 min) and was characterized via mass spectrometry (Figure S4). Similarly, the noncleavable control, Mal-PEG$_4$-BDT-4G, was synthesized by directly reacting BDT-4G with Mal-dPEG$_4$-NHS ester and TEA in dry DMSO (Scheme S3), and the product was purified via HPLC and characterized via mass spectrometry (Figure S5).

Synthesis of Cam-Mal-PEG$_4$-LVPRG-BDT-4G (ABC). To synthesize the cleavable ABC (Scheme S4), Cam-003 from a 1 mg/mL stock in 1× PBS (pH 7.4) was reacted with 4.2 equiv TCEP in 1× PBS supplemented with 5 mM EDTA for 2 h at 37 °C. Next, 10 equiv of Mal-PEG$_4$-LVPRG-BDT-4G from a 10 mg/mL stock in ultrapure water were added to the mixture, and the reaction was allowed to proceed overnight at room temperature. An excess of *N*-ethylmaleimide (50 equiv) was then added to cap the remaining free thiols, and the reaction proceeded for 1 h at room temperature. The mixture was then filtered twice using a 0.5 mL 30K MWCO centrifugal filter unit, and the absorbance of the recovered sample was measured at 280 nm to calculate the concentration.

MALDI-TOF MS. The drug conjugate (Mal-PEG$_4$-LVPRG-BDT-4G) and any intermediary compounds were prepared for MALDI-TOF MS analysis by mixing 1 mg/mL of the compound in acetonitrile/water with an equal volume of α-cyano-4-hydroxycinnamic acid (CHCA) matrix saturated in 50/50 acetonitrile/water with 0.1% TFA. Antibody samples were prepared by combining 1 mg/mL of the samples in water with an equal volume of sinapinic acid matrix saturated in 30/70 acetonitrile/water with 0.1% TFA. MALDI-TOF mass spectra were acquired using a Bruker AutoFlex MAX MALDI-TOF mass spectrometer (Bruker Biospin, Billerica, MA). The spectra were procured using FlexControl acquisition software in positive-ion reflectron mode for the drug conjugates (m/z range 200−3500) or positive-ion linear mode for the antibody samples (m/z range 30 000−200 000). Mass ranges were calibrated using a mixture of PEGs 1000, 2000, and 3000. The acceleration voltage was set to 20 kV. A total of 1000 individual laser shots were summed to provide the final spectrum. Spectra were processed using the FlexAnalysis software package, MestReNova, and GraphPad Prism.

Minimum Inhibitory Concentration (MIC) Assays. The MIC assays were performed as previously described with several modifications.[15] For the ABC MIC assay (Figures 3b and S12a), *P. aeruginosa* and Cam-Mal-PEG$_4$-LVPRG-BDT-4G were both incubated with 50% mouse serum, 64 units/mL thrombin, or the combined proteases from the onset of the experiment, and the indicated amounts of the proteases were present across all concentrations of the ABC. The BDT-4G MIC assay (Figures 3b and S12b) followed the same procedure as the ABC MIC assay, and the thrombin and mouse serum assays (Figure S13a,b) followed the previously described protocol.[15] To enumerate the CFU/mL from the serum MIC assay, aliquots from the well plate were diluted and plated onto an LB agar plate, and after overnight incubation, the colonies were counted to calculate the CFU/mL (Figure S13c).

Binding of ABCs to *P. aeruginosa*. *P. aeruginosa* isolate PAO1 was subcultured to mid-exponential phase, corresponding to an OD_{600} of 0.5. Cam-003, Cam-Mal-PEG$_4$-LVPRG-BDT-4G (cleavable ABC), and Cam-Mal-PEG$_4$-BDT-4G (noncleavable ABC) were then incubated with the bacteria at 62.5 nM for 1 h at 4 °C. Cells were washed once with 1× PBS, and then 62.5 nM DyLight 488-labeled goat anti-human secondary antibody (Abcam) was added to the samples. After incubating for 30 min at 4 °C, the cells were washed once and then fixed with 4% paraformaldehyde for 15 min at room temperature. The samples were washed twice and resuspended in 1× PBS for analysis using a FACSCalibur flow cytometer (BD Biosciences). The relative fluorescence intensity of the samples was determined from 25 000 events, and the data were analyzed with FlowJo and GraphPad Prism.

■ ASSOCIATED CONTENT

Supporting Information

The Supporting Information is available free of charge at https://pubs.acs.org/doi/10.1021/acsinfecdis.2c00492.

Experimental methods for detecting drug conjugate cleavage location and HIC, as well as reaction pathways, characterization of products, additional FRET assays, analysis of cleaved fragments, and antibacterial assays (PDF)

■ AUTHOR INFORMATION

Corresponding Author

Christopher A. Alabi − *Robert Frederick Smith School of Chemical and Biomolecular Engineering, Cornell University, Ithaca, New York 14853, United States;* orcid.org/0000-0003-2654-018X; Email: caa238@cornell.edu

Authors

Meghan K. O'Leary − *Robert Frederick Smith School of Chemical and Biomolecular Engineering, Cornell University, Ithaca, New York 14853, United States*

Asraa Ahmed − *Department of Chemistry and Chemical Biology, Cornell University, Ithaca, New York 14853, United States;* orcid.org/0000-0001-7222-268X

Complete contact information is available at: https://pubs.acs.org/10.1021/acsinfecdis.2c00492

Author Contributions

M.K.O. and C.A.A. conceptualized the research, designed the experiments, and analyzed the results. M.K.O. and A.A. performed the experiments. M.K.O. wrote the manuscript. All authors edited the manuscript. All authors have given approval to the final version of the manuscript.

Notes

The authors declare no competing financial interest.

■ ACKNOWLEDGMENTS

The authors thank Pavan Kumar Bangalore for synthesizing and purifying Fmoc-LVPRG-OH. This work was supported by the National Institutes of Health Award (R21-AI154102) and Cornell University's Center for Technology Licensing IGNITE: Research Acceleration funding program. This work made use of the Cornell Center for Materials Research

Facilities supported by the National Science Foundation under Award Number DMR-1719875.

REFERENCES

(1) Lewis, K. Platforms for Antibiotic Discovery. *Nat. Rev. Drug Discovery* **2013**, *12*, 371−387.
(2) Suzuki, M.; Kato, C.; Kato, A. Therapeutic Antibodies: Their Mechanisms of Action and the Pathological Findings They Induce in Toxicity Studies. *J. Toxicol. Pathol.* **2015**, *28*, 133−139.
(3) Hotinger, J. A.; May, A. E. Antibodies Inhibiting the Type III Secretion System of Gram-Negative Pathogenic Bacteria. *Antibodies* **2020**, *9*, 35.
(4) Ray, V. A.; Hill, P. J.; Stover, K. C.; Roy, S.; Sen, C. K.; Yu, L.; Wozniak, D. J.; Digiandomenico, A. Anti-Psl Targeting of *Pseudomonas Aeruginosa* Biofilms for Neutrophil-Mediated Disruption. *Sci. Rep.* **2017**, *7*, No. 16065.
(5) Motley, M. P.; Banerjee, K.; Fries, B. C. Monoclonal Antibody-Based Therapies for Bacterial Infections. *Curr. Opin. Infect. Dis.* **2019**, *32*, 210−216.
(6) Zaidi, T. S.; Zaidi, T.; Pier, G. B. Antibodies to Conserved Surface Polysaccharides Protect Mice against Bacterial Conjunctivitis. *Invest. Ophthalmol. Vis. Sci.* **2018**, *59*, 2512−2519.
(7) DiGiandomenico, A.; Warrener, P.; Hamilton, M.; Guillard, S.; Ravn, P.; Minter, R.; Camara, M. M.; Venkatraman, V.; MacGill, R. S.; Lin, J.; Wang, Q.; Keller, A. E.; Bonnell, J. C.; Tomich, M.; Jermutus, L.; McCarthy, M. P.; Melnick, D. A.; Suzich, J. A. A.; Stover, C. K. Identification of Broadly Protective Human Antibodies to Pseudomonas Aeruginosa Exopolysaccharide Psl by Phenotypic Screening. *J. Exp. Med.* **2012**, *209*, 1273−1287.
(8) Tabor, D. E.; Oganesyan, V.; Keller, A. E.; Yu, L.; McLaughlin, R. E.; Song, E.; Warrener, P.; Rosenthal, K.; Esser, M.; Qi, Y.; Ruzin, A.; Stover, C. K.; DiGiandomenico, A. Pseudomonas Aeruginosa PcrV and Psl, the Molecular Targets of Bispecific Antibody MEDI3902, Are Conserved Among Diverse Global Clinical Isolates. *J. Infect. Dis.* **2018**, *218*, 1983−1994.
(9) Jones, C. J.; Wozniak, D. J. Psl Produced by Mucoid Pseudomonas Aeruginosa Contributes to the Establishment of Biofilms and Immune Evasion. *mBio* **2017**, *8*, No. e00864-17.
(10) Mishra, M.; Byrd, M. S.; Sergeant, S.; Azad, A. K.; Parsek, M. R.; McPhail, L.; Schlesinger, L. S.; Wozniak, D. J. Pseudomonas Aeruginosa Psl Polysaccharide Reduces Neutrophil Phagocytosis and the Oxidative Response by Limiting Complement-Mediated Opsonization. *Cell. Microbiol.* **2012**, *14*, 95−106.
(11) Wu, M.; Maier, E.; Benz, R.; Hancock, R. E. W. Mechanism of Interaction of Different Classes of Cationic Antimicrobial Peptides with Planar Bilayers and with the Cytoplasmic Membrane of Escherichia Coli. *Biochemistry* **1999**, *38*, 7235−7242.
(12) Andersson, D. I.; Hughes, D.; Kubicek-Sutherland, J. Z. Mechanisms and Consequences of Bacterial Resistance to Antimicrobial Peptides. *Drug Resist. Updates* **2016**, *26*, 43−57.
(13) Fjell, C. D.; Hiss, J. A.; Hancock, R. E. W.; Schneider, G. Designing Antimicrobial Peptides: Form Follows Function. *Nat. Rev. Drug Discovery* **2012**, *11*, 37−51.
(14) Hancock, R. E. W.; Sahl, H.-G. G. Antimicrobial and Host-Defense Peptides as New Anti-Infective Therapeutic Strategies. *Nat. Biotechnol.* **2006**, *24*, 1551−1557.
(15) O'Leary, M. K.; Sundaram, V.; Lipuma, J. J.; Dörr, T.; Westblade, L. F.; Alabi, C. A. Mechanism of Action and Resistance Evasion of an Antimicrobial Oligomer against Multidrug-Resistant Gram-Negative Bacteria. *ACS Appl. Bio Mater.* **2022**, *5*, 1159−1168.
(16) Antoniak, S. The Coagulation System in Host Defense. *Res. Pract. Thromb. Haemost.* **2018**, *2*, 549−557.
(17) Böttger, R.; Knappe, D.; Hoffmann, R. Readily Adaptable Release Kinetics of Prodrugs Using Protease-Dependent Reversible PEGylation. *J. Controlled Release* **2016**, *230*, 88−94.
(18) Gallwitz, M.; Enoksson, M.; Thorpe, M.; Hellman, L. The Extended Cleavage Specificity of Human Thrombin. *PLoS One* **2012**, *7*, No. e31756.
(19) Claushuis, T. A. M.; de Stoppelaar, S. F.; Stroo, I.; Roelofs, J. J. T. H.; Ottenhoff, R.; van der Poll, T.; van't Veer, C. Thrombin Contributes to Protective Immunity in Pneumonia-Derived Sepsis via Fibrin Polymerization and Platelet−Neutrophil Interactions. *J. Thromb. Haemost.* **2017**, *15*, 744−757.
(20) Sun, H.; Wang, X.; Degen, J. L.; Ginsburg, D. Reduced Thrombin Generation Increases Host Susceptibility to Group A Streptococcal Infection. *Blood* **2009**, *113*, 1358−1364.
(21) Lee, C. J.; Ansell, J. E. Direct Thrombin Inhibitors. *Br. J. Clin. Pharmacol.* **2011**, *72*, 581−592.
(22) Wagner-Rousset, E.; Janin-Bussat, M.-C.; Colas, O.; Excoffier, M.; Ayoub, D.; Haeuw, J.-F.; Rilatt, I.; Perez, M.; Corvaïa, N.; Beck, A. Antibody-Drug Conjugate Model Fast Characterization by LC-MS Following IdeS Proteolytic Digestion. *mAbs* **2014**, *6*, 173−184.
(23) Farràs, M.; Román, R.; Camps, M.; Miret, J.; Martínez, Ó.; Pujol, X.; Casablancas, A.; Cairó, J. J. Heavy Chain Dimers Stabilized by Disulfide Bonds Are Required to Promote in Vitro Assembly of Trastuzumab. *BMC Mol. Cell Biol.* **2020**, *21*, 2.
(24) Dombach, J. L.; Quintana, J. L. J.; Nagy, T. A.; Wan, C.; Crooks, A. L.; Yu, H.; Su, C.-C.; Yu, E. W.; Shen, J.; Detweiler, C. S. A Small Molecule That Mitigates Bacterial Infection Disrupts Gram-Negative Cell Membranes and Is Inhibited by Cholesterol and Neutral Lipids. *PLOS Pathog.* **2020**, *16*, No. e1009119.
(25) Tsuchikama, K.; An, Z. Antibody-Drug Conjugates: Recent Advances in Conjugation and Linker Chemistries. *Protein Cell* **2018**, *9*, 33−46.
(26) Jackson, D. Y. Processes for Constructing Homogeneous Antibody Drug Conjugates. *Org. Process Res. Dev.* **2016**, *20*, 852−866.
(27) Brummel, K. E.; Paradis, S. G.; Butenas, S.; Mann, K. G. Thrombin Functions during Tissue Factor−Induced Blood Coagulation. *Blood* **2002**, *100*, 148−152.
(28) Lehar, S. M.; Pillow, T.; Xu, M.; Staben, L.; Kajihara, K. K.; Vandlen, R.; DePalatis, L.; Raab, H.; Hazenbos, W. L.; Hiroshi Morisaki, J.; Kim, J.; Park, S.; Darwish, M.; Lee, B.-C.; Hernandez, H.; Loyet, K. M.; Lupardus, P.; Fong, R.; Yan, D.; Chalouni, C.; Luis, E.; Khalfin, Y.; Plise, E.; Cheong, J.; Lyssikatos, J. P.; Strandh, M.; Koefoed, K.; Andersen, P. S.; Flygare, J. A.; Wah Tan, M.; Brown, E. J.; Mariathasan, S. Novel Antibody−Antibiotic Conjugate Eliminates Intracellular S. Aureus. *Nature* **2015**, *527*, 323−328.

https://doi.org/10.1021/acsinfecdis.2c00492
ACS Infect. Dis. XXXX, XXX, XXX−XXX